

NEW ASPECTS OF INDUSTRIAL CRYSTALLIZATION

KEN TOYOKURA

Department of Applied Chemistry, Waseda University, 3-4-1 Okubo,
Shinjuku-ku, Tokyo 169

Key Words: Industrial Crystallization, Crystallizer, Crystal Growth Rate, Design Theory, Secondary Nucleation

Industrial crystallization for the production of desired products, as expressed by produced crystal size and production rate, is discussed theoretically, and effective secondary nucleation and crystal growth rate are shown to be important. Recent studies on secondary nucleation rates are reviewed that involve complicated mechanisms and considered for application in design of crystallizers. Sticking phenomenon of suspended fines on growing crystals is discussed with regards to the population density of fines on the surface of growing seed. New mechanisms of crystal growth in an industrial crystallizer are also reviewed that involve breakage of growing crystal and sticking of suspended fines, and crystal growth rates available to calculate scaling up of a crystallizer is discussed.

Two kinds of design theories of continuous crystallizers are reviewed. One is proposed on an ideal models of states of crystal and solution in a crystallizer and the dimensionless characteristic factors defined by dimensionless crystal size and supersaturation, can be used, independently of system and product crystal size and shape. Another theory is proposed on product crystal, and is shown to be applicable to operational line, independently of size of a crystallizer under some restricted conditions.

Finally, industrial crystallization is becoming more and more important not only in conventional mass chemical processes, but also in fine chemical ones, and progressive studies on industrial crystallization will answer to the needs of the chemical industries in future.

Introduction

Industrial crystallization has been studied to propose chemical engineering theories on crystallization so that the desired product crystal is stably produced under reasonable operational conditions. Product crystals from industrial crystallizers are generally characterized by high purity and particular chemical and physical properties. Desired production from a crystallizer is quite often expressed by product crystal size (and size distribution) and production rate. They are correlated with suspension density of crystal, average effective nucleation and growth rate in a crystallizer under stable operation of a continuous crystallizer, as shown by the following equations (Toyokura, 1990b).

$$l_p = \int_0^{\theta_p} \left(\frac{dl}{d\theta} \right) d\theta + l_s = \left(\frac{dl}{d\theta} \right)_{l_{pav}} \cdot \theta_p + l_s \quad (1)$$

$$P = \rho_c \left(\frac{dL}{d\theta} \right)_{av} \cdot a = \rho_c \int_0^{l_p \max} k_v f(l) l_p^3 dl_p \quad (2)$$

$$a = \int_0^{l_p \max} k_a g(l) l^2 dl \quad (3)$$

$$V_t = \int_0^{l_p \max} k_v g(l) l^3 dl \quad (4)$$

$$V = V_t / (1 - \epsilon) \quad (5)$$

$$g(l) dl = \int_0^l f(l_p) d\theta_p \cdot dl_p \quad (6)$$

$$g(l_s) dl_s = \int_{\infty}^{l_s} f(l_p) d\theta_p \cdot dl_p = F d\theta \quad (7)$$

From Eqs. (1) and (2), product crystal size, or size distribution and production rate are easily understood to be correlated by nucleation and crystal growth rate. Retention time of a crystal in the crystallizer is also correlated with product crystal size and crystal growth rate, and the volume of the crystallizer is estimated by Eqs. (4), and (5). $l_{p \max}$, maximum size of product crystal, is also affected by crystal growth rate and retention time of crystals in the crystallizer, and $g(l)$ is correlated with effective nucleation rate F , through Eqs.(6) and (7). When stable operation is considered, Eqs. (3), (4) and (5) should be satisfied and these equations are restricted by the void fraction in stable operation in a crystallizer which is correlated by average effective nucleation rate for a unit volume of crystallizer, crystal growth rate, and retention. Therefore, nucleation and crystal growth rate in a crystallizer are considered to be important items for the design of a crystallizer and the crystallization process.

1. Secondary nucleation

Secondary nucleation is considered to dominate in a conventional industrial crystallizer, and has been studied much since the 1960's (Strickland-Constable, 1974). Toyokura and Yamazoe (1975) set up experimental equip-

* Received on June 1, 1995 Correspondence concerning this article should be addressed to K. Toyokura.

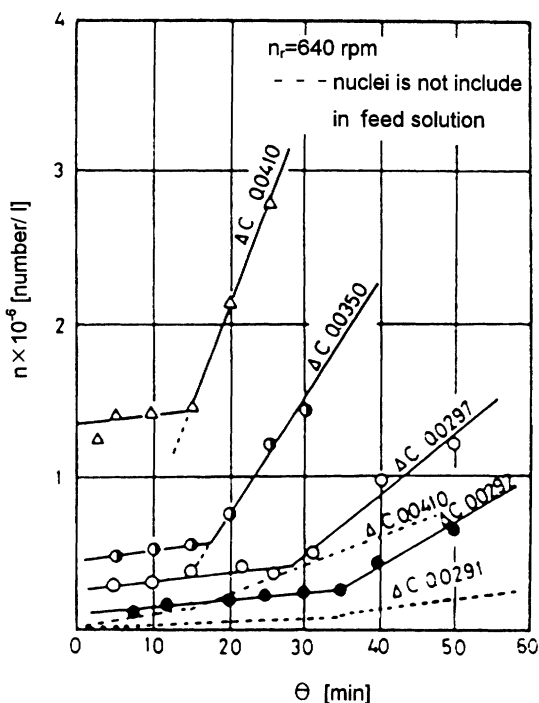


Fig. 1 Change in number of produced nuclei against sampling time at 640 rpm of agitator in a vessel

ment which was characterized by suspending seeds of a uniform size under homogeneous supersaturation, and generation rates of secondary nuclei formed by fluidized and stationary potassium alum seed crystals were observed and plotted on the two parallel lines (Aoyama and Toyokura, 1973). Nucleation rate obtained by fluidizing seeds were twelve times of that of stationary seeds, and Eqs.(8) and (9) were obtained.

For fluidizing seeds,

$$f_{flu}'' = 10 (\Delta C)^{3.3} (Re)^{2.5} \quad (8)$$

For fixed seeds,

$$f_{fix}'' = 0.85 (\Delta C)^{3.3} (Re)^{2.5} \quad (9)$$

Secondary nucleation rates by stationary seed crystals are considered to come from the fluid shearing stress of a supersaturated solution passed through the crystal bed, because there is no collision of seed crystals. In fluidizing a seed bed, crystals are suspended and collide with one another, and contact secondary nucleation tends to occur. When secondary nucleation rates by fluidizing seeds were compared with those of fixed bed in these equations, the effects of supersaturations and Reynolds' number on the secondary nucleation rate were almost same, and fluid shearing stress is supposed to dominantly affect secondary nucleation in the fluidized seed bed. In another test (Toyokura *et al.*, 1977), the supersaturated solution passed through a fluidizing seed bed, was fed into a vessel of a desired temperature, and kept for some time under agitation. In this solution, no fines were visible to the naked eye but some nuclei were supposed to be suspended. Then, the

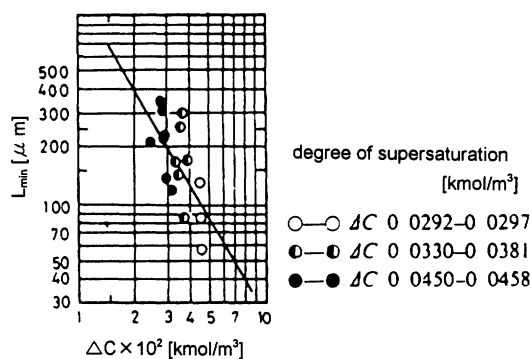


Fig. 2 Correlation of minimum size against supersaturation

solution was sampled into the sampling cell every five minutes and kept at the same temperature as operational supersaturation. While these sampled solutions were kept for several tens of minutes, fine crystals appeared and the in number counted in the sampling cell, n , were plotted against sampling times in Fig. 1. The counted numbers of fines gradually increased for some while. The number counted at the time of zero, was that of nuclei in the feed solution and increments of them were supposed to grow to become primary nuclei, born in the supersaturated solution in an agitated vessel. When nuclei were not included in the feed solution, the plots started from the origin of the coordinate axes and the slopes of them were the same as those in the same supersaturated solution. When the operation was kept longer in an agitated vessel, the number of observed fines increased more rapidly at the particular sampling time restricted by supersaturation. These rapid increases of fines are supposed to come from secondary nucleation generated by fines which were grown from nuclei. The sampling time at which the number of fines increased much is considered to be the time required for growth of nuclei to the minimum size of seed for secondary nucleation. Then the minimum seed sizes were calculated and plotted against an operational supersaturation in Fig. 2. The minimum seed size reported by Rousseau *et al.* (1976), was 180 to 190 μ for $MgSO_4 \cdot 7H_2O$, and is reasonably compared to the data in Fig.2. When product crystal size is discussed in terms of secondary nucleation for industrial purposes, the minimum size for secondary nucleation should be considered in terms of the operational supersaturation for product size and size distribution, and the correlation in Fig. 3 is available for this purpose. Secondary nucleation by minimum seed crystal was also observed and Eq.(10) was obtained.

$$f_{(min.)}'' = 6 \times 10^{-4} (\Delta C)^{3.3} n_r^3 \quad (10)$$

The effect of crystal seed size on secondary nucleation rate was studied through tests for secondary nucleation by agitated seeds in a crystallizer (Toyokura *et al.*, 1983b). Obtained data are shown in Fig. 4, and data from Garside and Jancic (1976) are also plotted for comparison. From these plots, the following equations are obtained for different sizes of seed.

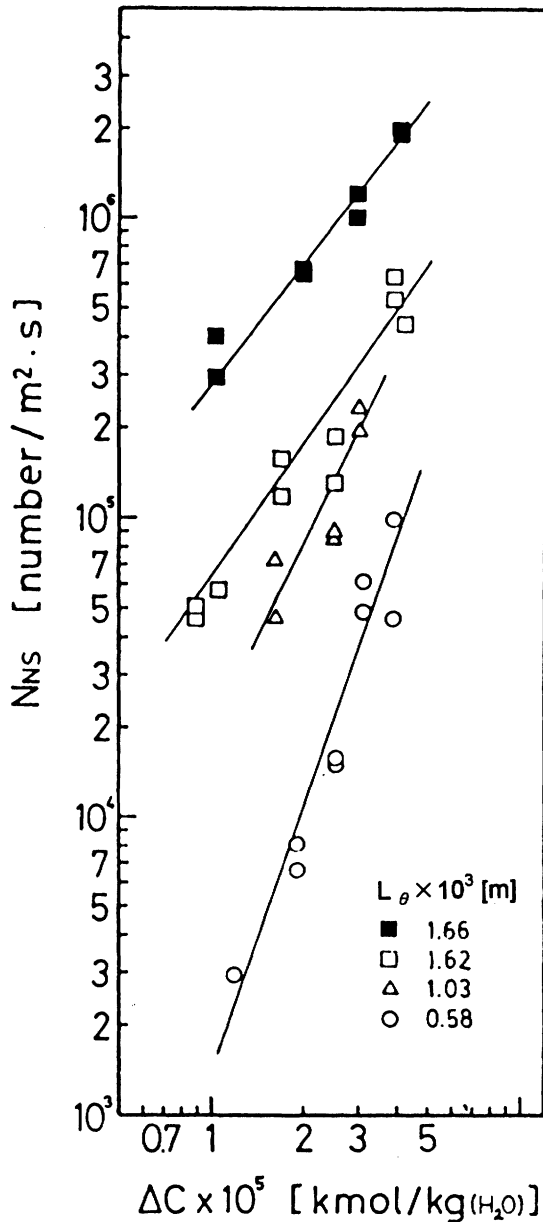


Fig. 3 Effect of supersaturation on nucleation rate (■: data from literature(Shirotsuka *et al.*, 1964))

$$\begin{aligned}
 f'' &= 6.9 \times 10^{11} \Delta C^{1.4} && \text{for seed size of } 1.62 \times 10^{-3} \text{ m} \\
 f'' &= 1.7 \times 10^{14} \Delta C^{2.2} && \text{for seed size of } 1.04 \times 10^{-3} \text{ m} \\
 f'' &= 1.3 \times 10^{18} \Delta C^{3.0} && \text{for seed size of } 0.58 \times 10^{-3} \text{ m} \quad (11)
 \end{aligned}$$

The secondary nucleation rates generated by crystal seeds of 0.58×10^{-3} m in size in Fig. 3 are a little larger than those estimated by Eq. (8) for fluidizing seeds, and the power numbers of supersaturation of these equations are almost same. They are plotted against crystal sizes in Fig. 4. In this figure, the power number of supersaturation of Eq. (10) for secondary nucleation rates by the minimum size seed is the same as that of Eq. (8). In that case, secondary nucleation rate on the case that fluid shearing stress is supposed to dominantly affect secondary nucleation. When seed crystal sizes became larger under agitated conditions, the power number of the correlative equation between crystal growth

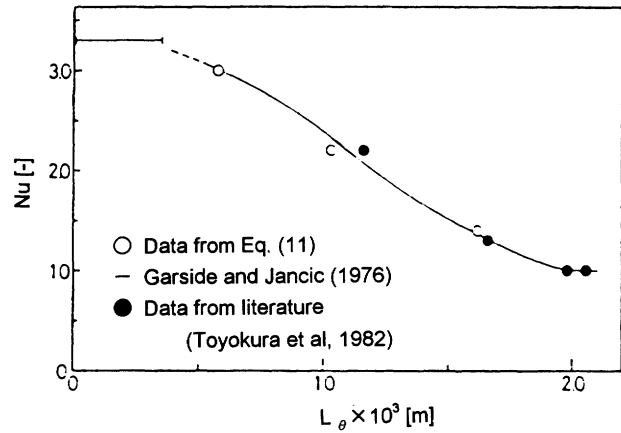


Fig. 4 Effect of seed size on power number of supersaturation

Table 1 Experimental value on n_N , n_G and calculated value of interfacial energy σ

System	σ [J/m ²]	n_N	n_G	n_N/n_G
CuSO ₄ ·5H ₂ O	10.5×10^{-3}	1.6	1.6	1.0
K-Alum	8.9×10^{-3}	3.3	1.6	2.0
MgSO ₄ ·7H ₂ O	7.3×10^{-3}	3.8	1.2	3.8

*Values obtained in experiment using fluidized bed with paddle type impeller (Toyokura *et al.*, 1979)

rate and supersaturation, decreased to 1.4.

Contact nucleation was reported to give some damage on seed crystal surfaces, and the repair of a damage surface was also discussed to affect continuing contact nucleation by Larson and Bending (1976). When this model is applied to discuss the correlative equation for contact nucleation rate, the time for regeneration of surface damage which is affected by crystal growth rate is supposed to be affected by contact nucleation rate, and then the new model, that the power number of the supersaturation in the correlative equation for contact nucleation rate, is almost the same as that for crystal growth rate. From this model, the power numbers of secondary nucleation rate are considered to suggest the contribution of shearing stress or crystal contact on secondary nucleation.

Secondary nucleation rates by fluidizing seed bed were also studied for the systems of MgSO₄·7H₂O and CuSO₄·5H₂O, and the same correlative equations were obtained (Toyokura *et al.*, 1980). Power number of these systems are also listed in Table 1. Interfacial energy on the crystal surface in supersaturated solution estimated by Nakai's method (Nakai, 1969) is also listed in it. From this table, the systems of more interfacial energy show less power number, and contribution of fluid shearing stress to secondary nucleation decreases on the same trend. In other words, contact nucleation is supposed to become more effective, and secondary nucleation of fluidizing CuSO₄·5H₂O seed is supposed to be affected more by contact nucleation.

The effect of an impeller agitation on a secondary nucleation rate was also studied by tests in which an agita-

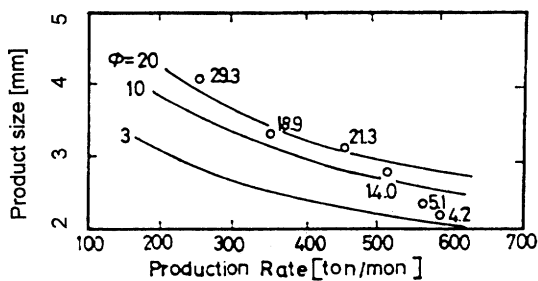


Fig. 5 Correlation between product size and production rate

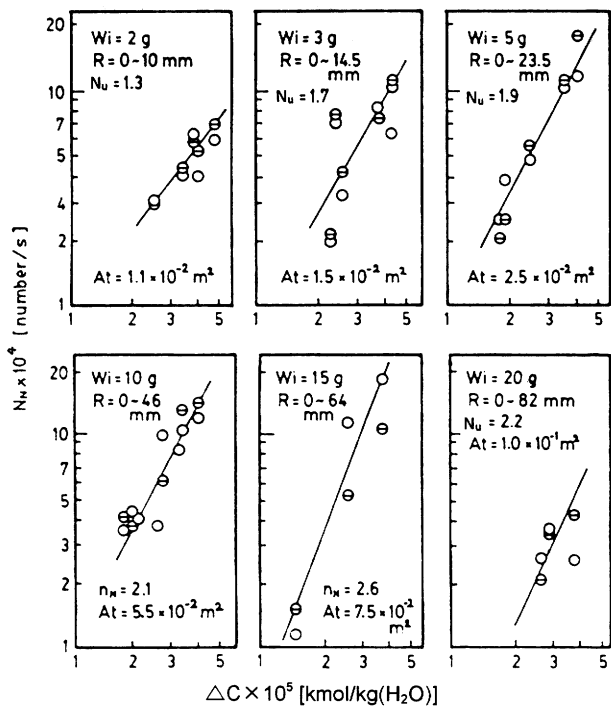


Fig. 6 Effect of supersaturation and amount of seed on nucleation rate (mixing time: 3 min. ○, 4 min. ●)

tor was set in fluidizing crystal bed (Toyokura *et al.*, 1979). Observed nucleation rates were correlated with supersaturation, ΔC , revolution rate n_γ , diameter of impeller d , and angle of impeller blade ϕ , as Eq.(12).

$$f'' = K (\Delta C)^{n_N} n_\gamma^3 d^4 (\sin \phi)^2 \quad (12)$$

n_N and K in equations were decided for several n_γ and d as followings for

$$\left. \begin{array}{l} n_\gamma = 0.5s^{-1} \quad d = 3 \times 10^{-2}m \\ n_\gamma = 0.67s^{-1} \quad d = 3 \times 10^{-2}m \\ \quad \quad \quad \quad d = 2.5 \times 10^{-2}m \\ \quad \quad \quad \quad d = 2 \times 10^{-2}m \end{array} \right\} N_u = 1.3, K = 6.7 \times 10^{19}$$

$$\left. \begin{array}{l} n_\gamma = 0.5s^{-1} \quad d = 2.5 \times 10^{-2}m \\ n_\gamma = 0.5s^{-1} \quad d = 2 \times 10^{-2}m \\ n_\gamma = 0.55s^{-1} \quad d = 2 \times 10^{-2}m \end{array} \right\} N_u = 1.6, K = 1.5 \times 10^{21}$$

From these correlative equations, the whole secondary nucleation rate in a crystallizer was supposed to be esti-

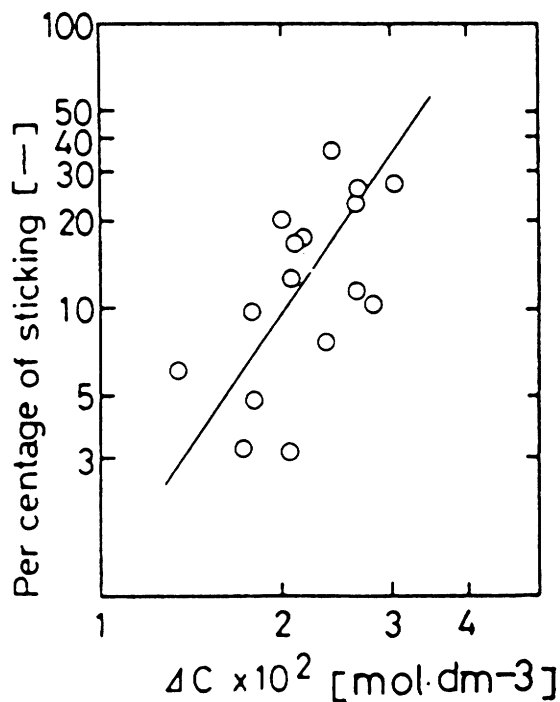


Fig. 7 Percentage of sticking of fines in fluidized crystals

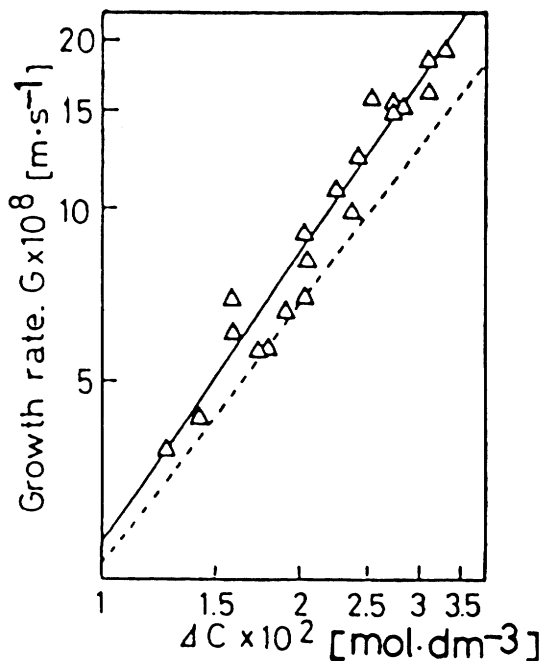


Fig. 8 Growth rate of potassium alum single crystal Δ : obtained in supersaturated solution with nuclei, ---: correlated in supersaturated solution without nuclei

mated by the sum total of local secondary nucleation rate. Data of production rate, product crystal size, and dimensionless supersaturation expressed by the ratio of supersaturation of the feed solution into the crystallizer to that of the outlet solution, was observed from operation of an industrial crystallizer for potassium alum (Toyokura *et al.*, 1976a). The crystallizer was a continuous cone fluidized bed type and the secondary nucleation rate in this crystallizer was estimated from data of laboratory tests

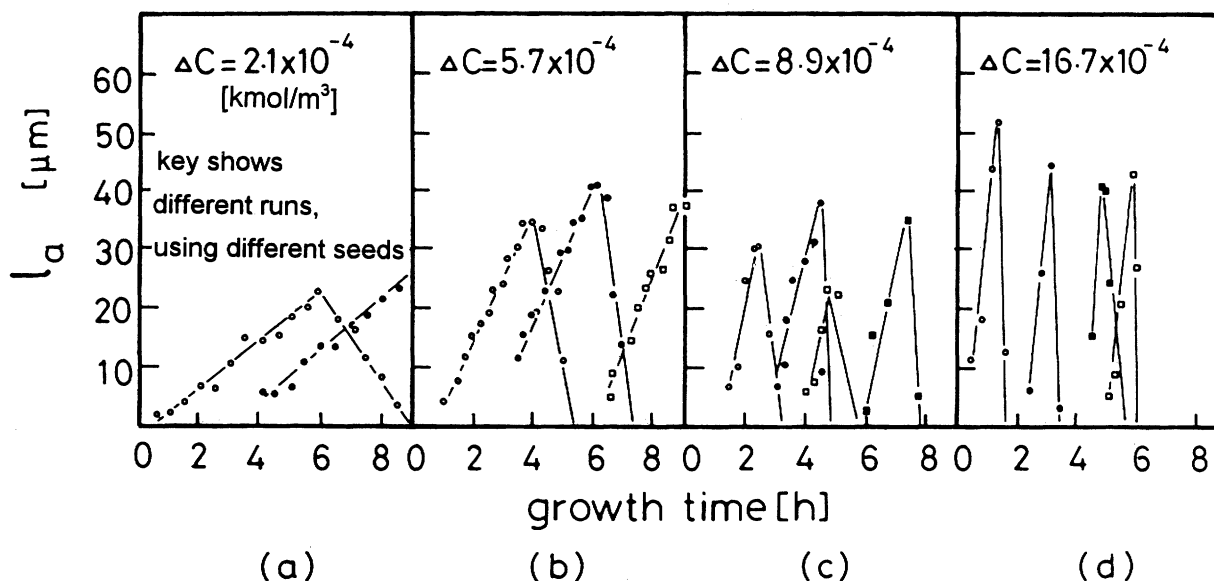


Fig. 9 Change of size, l_a of stuck fine crystals with growth time ($R = 50\text{min}^{-1}$)

correlated as Eq. (8) by the sum total method (Toyokura *et al.*, 1976b), and the estimated correlative lines among production rate, product size, and dimensionless supersaturation were obtained as lines in Fig. 5. Plots in this figure are data obtained from an industrial crystallizer, and agree with the estimated lines calculated by this model (Toyokura *et al.*, 1976a).

On the other hand, secondary nucleation rates in a continuous well mixed bed crystallizer were observed and compared with the values estimated from local nucleation rates calculated from Eqs. (8) to (12) by the sum total method. But the estimated values were very different from the observed ones and the difference was supposed to come from sticking of fines on suspended crystals (Toyokura *et al.*, 1982). In order to confirm this model, the following tests were done. Seed crystals were fluidized in a crystallizer in which contact nucleation by revolving impeller was taking place, and the height of the crystal fluidized bed was from 10 mm, which was the height of the revolving zone of the impeller, to 82 mm. These heights were changed by the amount of seed crystal from 2 to 20 g. The secondary nucleation rate increased with the amount of suspended crystals to 15g, but when the amount it became 20g, the secondary nucleation rate was much less than those obtained by other operational conditions as in Fig. 6 (Toyokura *et al.*, 1983a). In the other tests, a seed crystal of potassium alum was set in a flowing supersaturated solution in which alum fines were suspended (Toyokura *et al.*, 1986). When this seed crystal was watched through the microscope, it was easily observed to grow and some suspended fines fell down on the surface of the sampling cell. Parts of the fines on the surface, floated back into the flowing solution but other parts of them were stuck. Stuck fines were observed to grow up to some size. But the growth rate of seed crystal was faster than that of stuck fines, and the fines became buried in it after some operating period. In other words, many fines stuck on the surface

became incorporated into the seed crystals and disappeared completely. In these observations, some cracks of a length of several hundreds microns appeared suddenly on the surface of the growing seed crystal but these parts quickly grew and also disappeared soon. When the solution became undersaturated, the place on which cracks and stuck fines disappeared, dominantly dissolved. From these results, stuck fines and cracks are supposed to affect the quality of product crystals, even though they are not observed on the grown crystal surface.

Sticking phenomena of suspended fines on suspended seed crystals in a supersaturated solution were also studied for decrease of suspended fines by a method where the supersaturated solution passed through the fluidized seed crystal bed, and the percentage of stuck fines in the suspended ones was correlated against supersaturation in Fig. 7. The effect of suspended fines on the crystal growth rate was also shown as the data in Fig. 8.

In potassium alum and other soluble substance systems, it is not easy to observe those phenomena precisely because of quick growth rate. The crystal growth rate of SMC (s-carboxymethyl-cysteine) is much slower than those of soluble substances, and more detailed phenomena of sticking of fines on the growing crystal surface were studied through crystallization of SMC (Yokota and Toyokura, 1992). In this study, relatively large crystals with special marks were suspended together with other crystals and the behaviour of fines on the surface of the marked crystals was observed every fifteen minutes. The sizes of fines on the surface were changed as in Fig. 9, and the phenomenon was supposed to be the same as those of potassium alum. The number of stuck fines increased as in Fig. 10 and approached to a certain value which was restricted by supersaturation and revolution rate of an impeller. Other tests of sticking phenomena were studied by the use of crystallizer shown in Fig. 11 (Yokota and Toyokura, 1993a). In these crystallizing oper-

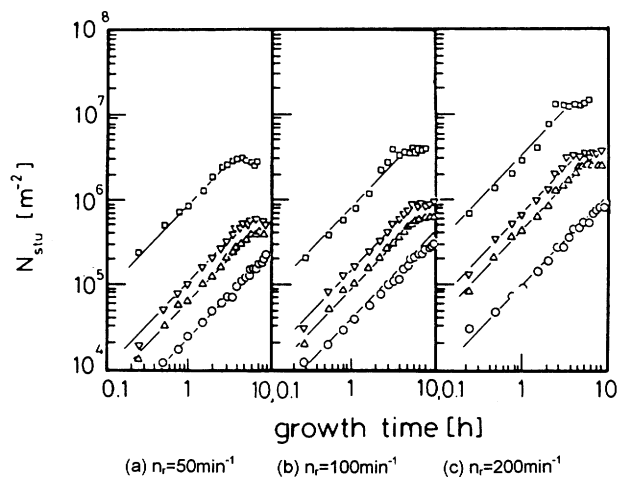


Fig. 10 Change in number of sticking fine crystals, N_{stu} with growth time (\circ : $\Delta C = 2.1 \times 10^{-4} \text{ kg} \cdot \text{kg}^{-1}$, \triangle : $\Delta C = 5.7 \times 10^{-4} \text{ kg} \cdot \text{kg}^{-1}$, ∇ : $\Delta C = 8.9 \times 10^{-4} \text{ kg} \cdot \text{kg}^{-1}$, \square : $\Delta C = 16.7 \times 10^{-4} \text{ kg} \cdot \text{kg}^{-1}$)

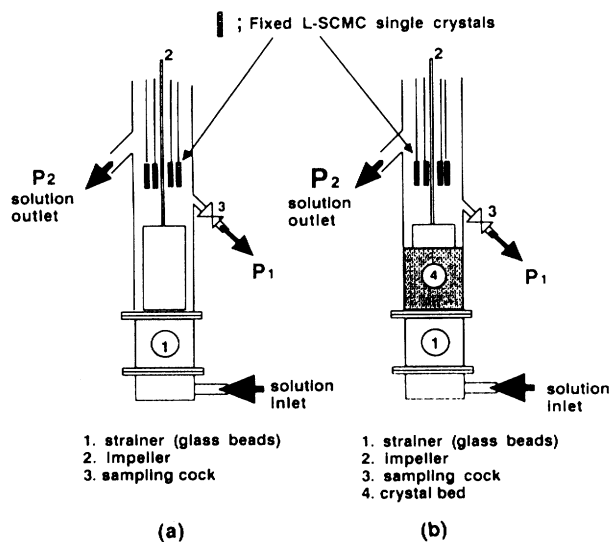


Fig. 11 Schematic illustration of crystallizers

ations, 2000 of L-SCMC seeds were fixed on stainless steel wires and a supersaturated solution was fed into the crystallizer. Secondary nuclei in equipment (a) are generated by fixed seed, but those in equipment (b) are generated by both an agitated crystal bed and a fixed seed bed in the crystallizer. The number of fines stuck on the growing surface of fixed seeds was observed against growing periods and the data from equipment (a) were plotted in **Fig. 12**. When plots in this figure are compared in the initial stage of both tests, an increasing rate of fines sticking was affected by operating supersaturation, independently of flow rate and suspension density of fines in the supersaturated solution. The increase of number of fines on the surface is supposed to come from surface nucleation on the fixed seeds. When the operations were continued for some while, an increase in stuck fines became affected by flow rate and suspension density of fines in the supersaturated solution. Seeds fixed on the wire were preliminarily made in a stationary low supersaturated solution and fines rarely were

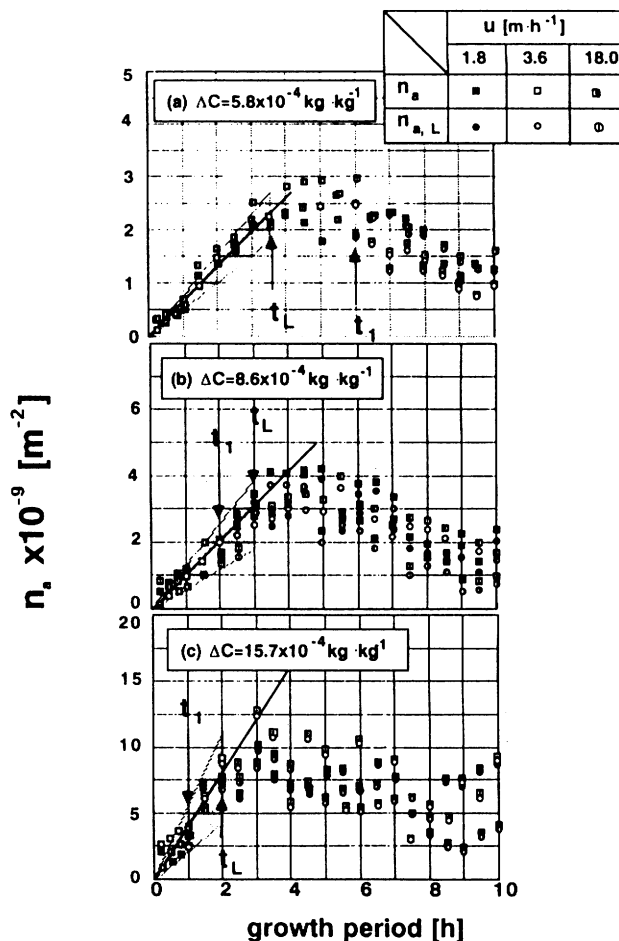


Fig. 12 Time course of number density of fine D-SCMC, n_a and L-SCMC, n_{aL} , on L-SCMC seed obtained from equipment (a)

on their surfaces, as shown in **Fig. 10**. From these results, the sticking phenomena of fines on the surface of growing crystals were supposed to be affected by number density of the fines on the surface. Estimated numbers of effective nucleation rates by fluidized seed bed were applied for design of a continuous fluidized bed cone crystallizer, but estimated numbers by agitated multi seed were different from observed values, as mentioned before. These differences are supposed to come from the number density of the surface of growing crystals.

2. Crystal Growth Rate

Crystal growth rates were observed by tests of a single fixed crystal (Shirotsuka *et al.*, 1964), fluidized (Toyokura *et al.*, 1980), and agitated multi crystals (Shirotsuka *et al.*, 1968), and discussed with conventional crystal growth theories. Crystal growth of multi suspended crystals in a crystallizer is affected by suspended fines grown from nuclei (Toyokura *et al.*, 1986). Crystal growth rates of L-SCMC seed crystals were studied on number density of fines on the surface of a growing crystal and correlations in **Fig. 13** were obtained (Yokota and Toyokura, 1993b). Crystal growth rates of a particular shape crystal, such as needle and flat disk, were also stud-

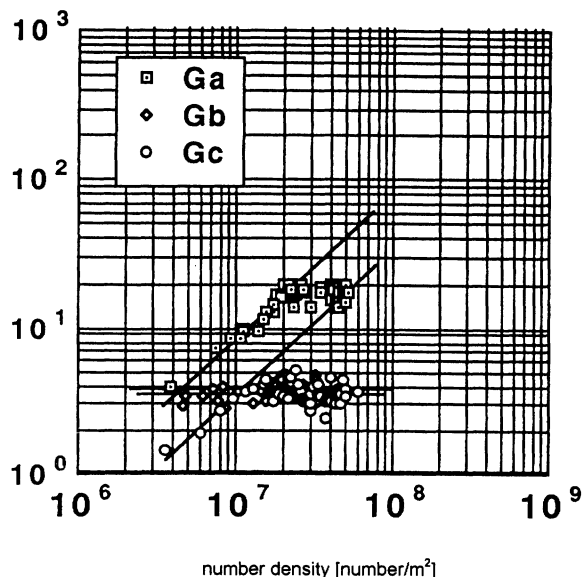


Fig. 13 Correlation between growth rate G and number density n of fines $\Delta C = 5.8 \times 10^{-4}$ (SCMC) kg/kg (water)

ied for gypsum (Toyokura *et al.*, 1987a, and Toyokura *et al.*, 1990a) or urea (Toyokura and Ohki, 1989), and barium hydroxide octahydrate crystal (Toyokura *et al.*, 1984). When needle crystal grew in a supersaturated solution under agitation, the longitudinal length was broken quite often, but latitudinal long the grew without being broken. Therefore, the crystal shapes expressed by the ratio of both lengths, were changed complexly with the growth of needle crystal. When many crystals were suspended in a crystallizer, the ratio of both lengths was proposed to be estimated by a simple model equation (Toyokura and Ohki, 1989). Crystal growth of flat disk crystals in a supersaturated solution was characterized by dominant appearances of fines on the flat surface, and these fines grew without being buried into a grown part of the flat surface (Toyokura *et al.*, 1984).

When crystal growth rate is applied for design of an industrial crystallizer characterized by multi suspended crystals the, effects of suspended fines and embryos of the crystallizing component in a supersaturated solution and surface nucleation on the growing crystal surface should be considered. Actually, these items are supposed to affect the surface reaction step of the crystal growth mechanism, and an average crystal growth rate used in Eqs.(1) and (2), is supposed not to be much affected by scaling up when average supersaturation and maximum supersaturation in crystallizers were kept in the a same range. Therefore, crystal growth rates observed by laboratory tests might be available for design of industrial crystallizers.

3. Design Theories of Continuous Crystallizers

Design theories are generally proposed on two different stand points, (A) and (B) .

Case (A) : Behaviors of crystal and solution in a crystallizer are assumed to be expressed in ideal states, and the

Table 2 Classification of continuous crystallizers

ideal behavior		model	corresponding actual crystallizer
crystal	solution		
well mixed	piston	conveying bed	D.T.B. type
well mixed	well mixed	well mixed bed	well stirred tank type
piston	piston	classified bed	Krystal-Oslo type
piston	well mixed	classified bed	Krystal-Oslo type

produced crystal size and amount are calculated from these ideal models in a crystallizer. The correlative equations are derived from model behaviors of these items, and a crystallizer is designed for a desired product using these correlative equations.

Case (B) : Final product is expressed by Eqs.(1) and (2), and actual volume of a crystallizer is decided from laboratory test data by the same type of crystallizer.

3.1 Design theories for ideal model crystallizers

Solid and liquid phases coexist in a crystallizer, and ideal behaviors of both phases are considered to be well mixed or the piston flow states. Therefore, four different types of crystallizers are classified as in Table 2.

a) Design theories for conveying bed type crystallizer (Shirotsyka and Toyokura, 1971)

The ideal model for a conveying type crystallizer is that crystals are circulated with flowing solution without mixing. For this crystallizer, crystal seeds and solution are fed into the crystallizer by F^1 and F , respectively, and the solution passed through the crystallizer, decreasing its concentration. The solution is removed from the crystallizer when it reaches the outlet of the crystallizer. But crystal seed gradually grows up to a product size l_2 in circulating supersaturated solution and then the grown crystal is taken out as product. When crystal growth rate in this crystallizer is assumed to be proportional to supersaturation, the volume of the crystallizer, V^1 , is correlated with a crystal growth rate, a production rate and a product crystal size by Eqs.(13)- (15),

$$V^1 = A_{C.B.V.} \times (C.F.C.)_{C.B.V.} \quad (13)$$

$$A_{C.B.V.} = \frac{P_2 l_2}{4 (dl/d\theta)_{\max} \rho_c (1 - \epsilon)} \quad (14)$$

$$(C.F.C.)_{C.B.V.} = \frac{(1 - X_1^4)}{1 - 1/\phi} \quad (15)$$

$A_{C.B.V.}$ defined by Eq. (14) is the design factor and estimated from the production rate, P_2 , the product crystal size, l_2 , the maximum crystal growth rate corresponding to the maximum supersaturation in a crystallizer, $(dl/d\theta)_{\max}$, and operating suspension density of crystal, $1 - \epsilon$ ($C.F.C.)_{C.B.V.}$, defined by Eq. (15) is the characteristic factor for crystallization, and is a dimensionless number independent of a system, production rate, crystal size and shape. x_1 and ϕ in Eq. (15) are dimensionless crystal size, (the ratio of a seed crystal size to a product one) and a dimensionless super-

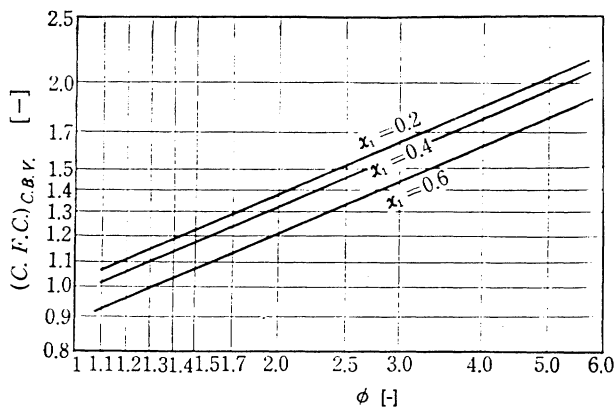


Fig. 14 Correlation of $(C.F.C.)_{C,B,V}$ against ϕ and x

saturation, (the ratio of supersaturation of feed solution to that of outlet one respectively). Therefore, $(C.F.C.)_{C,B,V}$ is easily expressed by a dimensionless chart as shown in Fig. 14, where $(C.F.C.)_{C,B,F}$ is plotted against ϕ with x_1 as a parameter. Circulating flow rate of a solution in a conveying bed type crystallizer, F , is also estimated by Eq. (16), and the design factor $A_{C,B,F}$ and $(C.F.C.)_{C,B,F}$ are also defined by Eqs. (17) and (18).

$$F = A_{C,B,F} \times (C.F.C.)_{C,B,V} \quad (16)$$

$$A_{C,B,F} = P_2 / M \Delta C_1 \quad (17)$$

$$(C.F.C.)_{C,B,F} = (1 - x^3) / (1 - 1/\phi) \quad (18)$$

When V' and F are calculated, the sectional area, s , and the height of a crystallizer, z , are easily obtained by Eqs. (19) and (20).

$$S = F / c'u \quad (19)$$

$$z = V' / s \quad (20)$$

b) Design theory for a well mixed bed type crystallizer (Shirotsuka *et al.*, 1968)

The volume, V , of a crystallizer on solvent basis required for production rate, P_2 , and a dominant product crystal size, l_d , is obtained by Eq. (21) for the case that solution and crystal in a crystallizer are mixed well.

$$V = A_{W,M,B} \times (C.F.C.)_{W,M,B} \quad (21)$$

Here, $A_{W,M,B}$ and $(C.F.C.)_{W,M,B}$ are shown by Eqs. (22) and (23), respectively,

$$A_{W,M,B} = P_2 l_d / (dl/d\theta)_{av} \cdot M(\Delta C_1) \quad (22)$$

$$(C.F.C.)_{W,M,B} = \frac{\phi(1_1^2 + 2/3x_1 + 2/9)}{(1 - 1/\phi)(x_1^3 + x_1^2 + 2/3x_1 + 2/9)} \quad (23)$$

When V is decided, the actual volume of a crystallizer V' becomes Eq. (24).

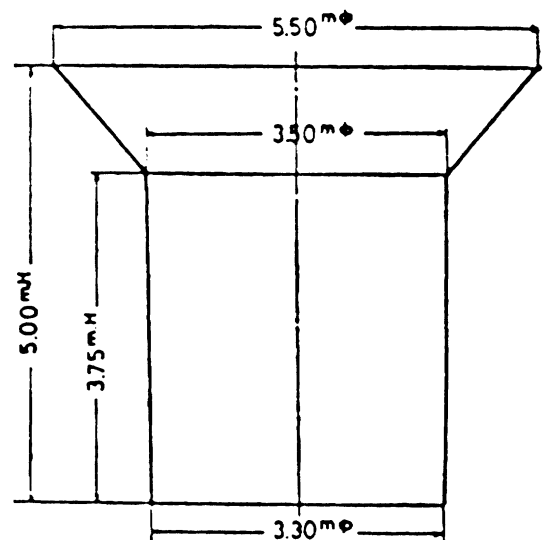


Fig. 15 Wall shape of DAIDOH type crystallizer simplified from cone type

$$V' = \frac{V(\rho_v + M C_{av})}{\epsilon \rho_u} \quad (24)$$

c) Design theories of a fluidized bed type crystallizer

In a continuous fluidized bed type crystallizer, crystals drop down slowly from the top to the bottom, fluidizing at the particular height decided by hydrodynamics of a fluidized bed, and a supersaturated solution is fed into the bottom and goes up through the crystallizer. From this model, the height of the crystallizer, z , was proposed to be estimated by the following equations (Shirotsuka *et al.*, 1965).

For the case of crystal growth rate controlled by the diffusion step

$$z = \frac{\alpha_D P_2 \cdot l_2^{4/3} (C.F.D.) L_n \phi}{\Delta C_1} \quad (25)$$

For the case of a crystal growth rate controlled by the surface reaction step

$$z = \frac{\alpha_R P_2 l_2 (C.F.SR.) L_n \phi}{\Delta C_1} \quad (26)$$

Here $C.F.D.$ and $C.F.SR.$ are the characteristic factor for diffusion step, and the characteristic factor for surface reaction step, respectively, and defined by Eqs. (27) and (28).

$$C.F.D. = \int_1^{y_1} \frac{\phi y^{3/3} dy}{(1 - \epsilon_2 y^{-1/3}) \{1 + (\phi - 1)(y^3 - 1)/(y_1^3 - 1)\} L_n \phi} \quad (27)$$

$$C.F.SR. = \int_1^{y_1} \frac{\phi y^3 dy}{(1 - \epsilon_2 y^{-1/3}) \{1 + (\phi - 1)(y^3 - 1)/(y_1^3 - 1)\} L_n \phi} \quad (28)$$

Pilot plant tests for crystallization of sodium sulphate were carried out, and obtained data were plotted with Eq. (25) or (26). The design constant α_D was decided from

Table 3 Operational data of DAIDOH type of B

Run	$P \times 10^3$ kg/h	$d_{p1} \times 10^4$ m	$d_{p1} \times 10^4$ m	$\Delta C_1 \times 10^2$ kmol/m ³ (H ₂ O)	$\Delta C_2 \times 10^2$ kmol/m ³ (H ₂ O)	Z _{obs} m	temperature °C	Z _{cal} m
3-1	3.72	10.30	3.65	3.14	1.50	4.48	60.1	4.65
3-2	3.89	11.00	3.52	2.95	1.36	4.68	61.2	4.60
3-3	3.55	13.00	2.93	2.87	1.40	4.93	59.6	4.20
3-4	3.65	11.00	3.57	2.96	1.43	4.65	58.4	4.60
3-5	3.92	10.00	3.74	3.15	1.45	4.52	60.4	4.20

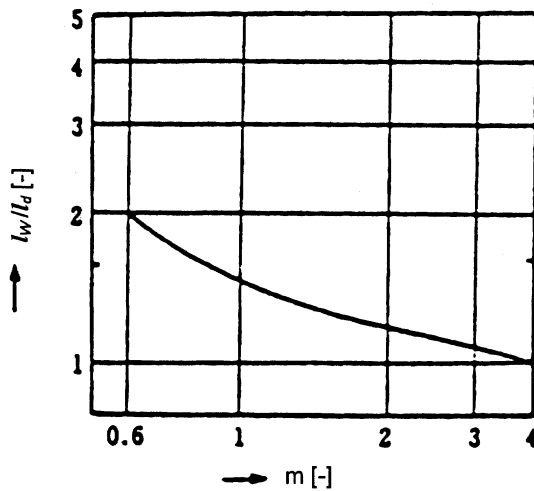


Fig. 16 Correlation between m and l_w/l_d

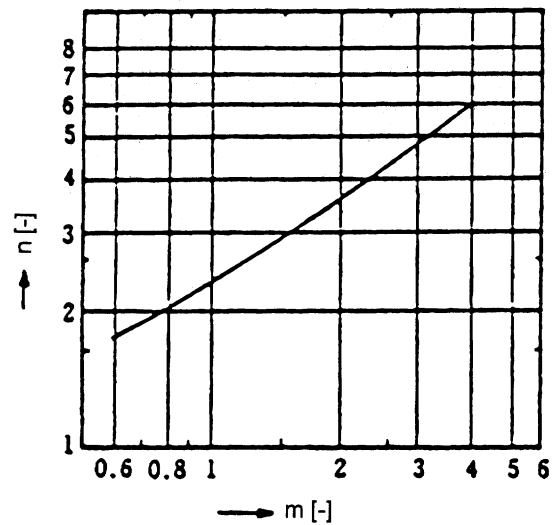


Fig. 17 Correlation between m and n

comparison between the correlative line for α_D and that for α_R , and used for discussion on industrial data of classified cone crystallizers (Aoyama and Toyokura, 1973). On these discussions, comparison between the observed height of a fluidized bed of industrial crystallizers shown in Fig. 15 and those estimated by these design equations were done, as shown by z_{obs} and z_{cal} in Tables 3.

3.2 Design theory based on production rate and product crystal size distribution

The size distribution of crystals produced by an industrial crystallizer is different from homogeneous or classified on and quite often expressed by the Rosin-Rammler equation. Then, product crystal size distribution, $f'(l_p)$, in Eqs.(2), (6) and (7) is considered to be replaced by the Rosin-Rammler equation. Therefore, crystal size distribution γ is considered to be expressed by Eq. (29).

$$\gamma = \exp^{-(l/l^*)^m} \quad (29)$$

Here, γ is a relative cumulative amount of a product crystal on population basis, and m is a uniformity number. l^* is the particular size of crystal corresponding to γ of 0.3679. When a dimensionless size x is defined as l/l^* , product size distribution $f'(l)$ becomes Eq.(30).

$$f'(l) = \left| \frac{d\gamma}{dl} \right| = x^{m-1} e^{-x^m} \quad (30)$$

Therefore, the dominant size of crystal l_d of this size distribution becomes Eq. (31).

$$x_d = \left(1 + \frac{2}{m}\right)^{1/m} \quad (31)$$

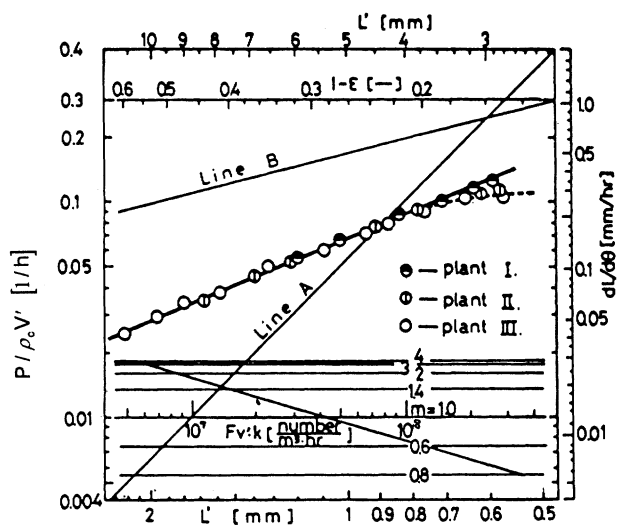


Fig. 18 Design chart diagram of ammonium alum operation data

Then, two important equations, Eqs. (32) and (33), are derived for expression of a stable continuous operation (Toyokura and Sakai, 1987b).

$$\frac{P}{\rho_c V} = l^{*3} F_v k_p m \int_0^\infty x^{m+2} e^{-x^m} dx \quad (32)$$

$$\frac{P}{\rho_c V} = (1 - \epsilon) \left(\frac{dl}{d\theta} \right)_{av} \left/ \left\{ \frac{l^* \int_0^\infty x^m e^{-x^m} dx \int_0^\infty x^3 e^{-x^m} dx}{\int_0^\infty e^{-x^m} dx \int_0^\infty x^{m+2} e^{-x^m} dx} \right\} \right. \quad (33)$$

When crystal size distribution is expressed by weight basis as in Eq. (34), l_w and n corresponding to l^* and n , are correlated by Figs. 16 and 17.

$$R = \exp \{-(l/l_w)^n\} \quad (34)$$

When these theories were applied for plotting of data obtained from tests of a laboratory, a pilot plant and an industrial crystallizer, these plots lay on the particular operating line in design chart in Fig.18 (Aoyama *et al.*, 1982). From these plots, when the particular operating line is obtained from tests of continuous laboratory equipment of a selected type, the volume of an industrial crystallizer required for the desired amount and size of product crystal is easily decided. The same kinds of treatment were applied for forty-eight systems (Aoyama *et al.*, 1988) and became popular for industrial purposes. Ideal design theories treated in 4.1 are special cases for $m = 1$ or ∞ in Eqs. (32) and (33), and the design chart in Fig.18 is easily applied for decision of operational conditions for production of different size crystals and other necessary properties, on additions of decision of the required volume of a crystallizer.

4. Further Development of Industrial Crystallization

The working party on crystallization was organized by the European Federation of Chemical Engineering in 1969, and the study group of the industrial crystallization started at the Society of Chemical Engineers Japan in April 1969. Study on industrial crystallization is in progress. New industrial crystallization theories for secondary nucleation and crystal growth rate, have been studied much, and design theories applicable for industrial purposes also have been proposed. Recently, tailor made habit modifiers and polymorphism have been studied, and particular crystallizing processes are able to be easily developed for production of special desired products. In the chemical industries, energy saving production processes are required to be developed, and high products yield is also desired. Generally, crystallization is characterized by less latent heat of phase transformation and production of stable functional crystals of a desired component. Industrial crystallization is adopted mainly in food processing, pharmaceuticals, but also in other industries. For commodity chemicals that are mass produced, substances of high quality should be produced for less cost, and reasonable design of crystallizers and operational conditions is becoming more and more important. Additionally, by-products from chemical industries and recovery products from the environmental purification processes are often obtained as crystals, which could be reused for raw materials. When chemical industries in the near future are considered, industrial crystallization is expected to become available to produce highly functional substances at a reasonable cost with effective use of waste materials, and continuing research will likely respond to the demands of future chemical industries.

Nomenclature

A	: design factor decided by production rate, product size, growth rate and suspension density	[m ³]
A _t	: total crystal surface area	[m ²]
a	: crystal surface area per volume of a crystallizer	[m ² /m ³]
C*	: concentration of solution	[m ³ (solvent)/m ³]
C.F.C.	: characteristic factor for crystallization	[-]
C.F.D.	: characteristic factor on crystallization in classified bed type on diffusion control case	[-]
C.F.S.R.	: characteristic factor on crystallization in classified bed type on surface reaction control	[-]
ΔC	: supersaturation	[kmol·kg ⁻¹ (H ₂ O) or kmol·m ⁻³]
d	: impeller diameter	[m]
F	: flow rate of solution	[m ³ /h]
F*	: nucleation rate of effective nuclei	[number/sec]
f	: secondary nucleation rate per unit surface area of seed crystal	[number/m ² sec]
f'(l)	: feed or removal rate of number of crystal of size "l" from crystallization	[number/sec, m ²]
G	: growth rate (suffix a, b, c shown direction)	[m/h]
g(l)	: number of crystal of size "l" suspended in a crystallizer	[number,m]
K	: constant for correlation for secondary nucleation	[-]
k	: shape factor	[-]
L	: crystal size obtained by the ratio of crystal volume to crystal surface area	[m]
l	: crystal size	[m]
l ₂	: crystal size at the top of the bed	[m]
l _d	: dominant size of crystal	[m]
l _w	: dominant size	[m]
M	: molecular weight	[kg/kmol]
m	: uniformity number on population base plot	[-]
N _u	: power number of supersaturation for secondary nucleation rate	[-]
N _{NS}	: secondary nucleation rate per a volume of crystallizer	[number/m ³ ·s]
N _N	: secondary nucleation rate	[number/s]
n	: number of fines	[number]
n	: uniformity number on weight base plot	[-]
n _G	: power number of supersaturation in a correlative equation for crystal growth rate	[-]
n _r	: rotational speed of impeller	[s ⁻¹]
P	: production rate	[g/s]
R	: relative cumulative weight of product crystal	[-]
Re	: Reynolds number based on crystal size	[-]
S	: sectional area of crystallizer	[m ²]
u	: superficial velocity	[m/s]
V _t	: volume of crystal suspended in a crystallizer	[m ³]
V'	: actual volume of a crystallizer (= volume of slurry in a crystallizer)	[m ³]
x	: dimensionless crystal size for conveying and well mixed bed type	
y	: dimensionless crystal size for classified bed type	
z	: height of crystallizer	[m]
α	: design constant for continuous fluidized bed type crystallizer	
γ	: relative cumulative number of product crystal	[-]
ε	: void fraction	[-]
θ	: time, retention time of crystal in a crystallizer	[sec]
ρ	: density	[g/m ³]
σ	: interfacial energy on surface of growing crystal	[J/m ²]
φ	: angle of impeller blade	[rad]
φ	: dimensionless supersaturation expressed by the ratio of maximum value to minimum one	[-]
<Subscript>		
a	: surface	
av	: average	

C.B.F	: circulation flow for conveying bed type
C.B.V.	: volume for conveying bed type
c	: crystal
D	: diffusion control
la	: size of stuck fines
max	: maximum value
p	: product
R	: surface reaction control
s	: seed
stu	: stuck fines on surface of growing crystal
u	: solution
v	: volume, solvent
W.M.B	: well mixed bed type
1	: feed for conveying or mixed bed type, bottom for fluidized bed type
2	: outlet at top of bed

Literature Cited

- Aoyama, Y. and K. Toyokura; "Crystallization of Sodium Sulfate by Classified-Bed Type Crystallizer—Scaling-up for Industrial Plant from Pilot Data—," *Kagaku Kogaku*, **37**, 416-421 (1973)
- Aoyama, Y., G. Kawakami, T. Mukaida and K. Toyokura; "Crystallization Phenomena of Alum and Other Substances in CEC Type Crystallizer," *Ind. Crystallization* '81, 199-208, North Holland Pub., The Netherlands (1982)
- Aoyama, Y., H. Miki and K. Toyokura; "Correlation between Productivity and Size of Crystals in a Continuous Industrial Crystallizer," *Ind. Crystallization* '87, 337-341, Elsevier Sci. Pub., The Netherlands (1988)
- Garside, J. and S. J. Jancic; "Measurement and Scale-up of Secondary Nucleations Kinetics for the Potash Alum-water System," *AIChE J.*, **25**, 948-958 (1976)
- Larson, M. A. and L. L. Bending; "Nuclei Generation from Repetitive Contacting," *AIChE Symp. Ser.*, **72**, 21-29 (1976)
- Nakai, T.; "Studies of the Estimation of the Interfacial Energy of Embryo in Solid-liquid Systems," *Bulletin of the Chem. Soc. Japan*, **42**, 2143-2148 (1969)
- Rousseau, R. W., K. K. Li and W.L. McCabe; "The Influence of Seed Crystal Size on Nucleation Rate," *AIChE Symp. Ser.*, **72**, 48-52 (1976)
- Shirotsuka, T., K. Toyokura and K. Matsumoto; "Rate of Crystal Growth from Aqueous Ammonium Chloride Solution Added with Urea and/or Lactose," *Kagaku kogaku*, **28**, 221-227 (1964)
- Shirotsuka, T., K. Toyokura and Y. Sekiya; "Method for Calculating the Height of the Continuous Classified-bed Type Crystallizer," *Kagaku kogaku*, **29**, 698-704 (1965)
- Shirotsuka, T., K. Toyokura and F. Sugiyama; "Design Method of Continuous Well Stirred Tank Type Crystallizer," *Kagaku Kogaku*, **30**, 833-839 (1968)
- Shirotsuka, T. and K. Toyokura; "Design of Continuous Crystallizers," *Chem. Eng. Prog. Symp. Ser.*, **67**, 145-153 (1971)
- Strickland-Constable R.F; "The Breeding of Crystal nuclei—a Review of the Subject," *AIChE Symp. Serie.*, **68**, 1 (1974)
- Toyokura, K. and K. Yamazoe; "Secondary Nucleation Rate of Aluminum Potassium Sulfate Dodecahydrate," *Kagaku Kogaku Ronbunshu*, **1**, 262-266 (1975)
- Toyokura, K., N. Yago, Y. Yamazoe and Y. Aoyama; "Design Method of Crystallizers Based on Secondary Nucleation Rate," *Kagaku Kogaku Ronbunshu*, **2**, 561-565 (1976a)
- Toyokura, K., K. Yamazoe and J. Mogi; "Secondary Nucleation Rate of Alum in a Fluidized Bed," *AIChE Symp. Ser.*, **72**, 53-60 (1976b)
- Toyokura, K., J. Mogi and I. Hirasawa; "Secondary Nucleation of K-alum by Minimum Size Seeds in a Stirred Vessel," *J. Chem. Eng. Japan*, **10**, 35-39 (1977)
- Toyokura, K., M. Uchiyama, I. Hirasawa and M. Kawai; "Effect of Collision by Agitation of Impeller on Secondary Nucleation Rate of K-alum," *Kagaku Kogaku Ronbunshu*, **5**, 596-600 (1979)
- Toyokura, K., H. Sato, M. Uchiyama and K. Tawa; "Rate of Secondary Nucleation Generated from Fluidized Seeds of $\text{CuSO}_4 \cdot 5\text{H}_2\text{O}$ System and $\text{MgSO}_4 \cdot 7\text{H}_2\text{O}$ System," *Kagaku Kogaku Ronbunshu*, **6**, 602-608 (1980)
- Toyokura, K., M. Uchiyama, M. Kawai, H. Akutsu and T. Ueno; "Secondary Nucleation of $\text{KAl}(\text{SO}_4)_2 \cdot 12\text{H}_2\text{O}$, $\text{MgSO}_4 \cdot 7\text{H}_2\text{O}$ and $\text{CuSO}_4 \cdot 5\text{H}_2\text{O}$," *Ind. Crystallization* '81, 87-96, North-Holland Pub. (1982)
- Toyokura, K., H. Akutsu, M. Kawai, and M. Uchiyama; "Secondary Nucleation of K-alum Crystals above the Stirring Zone in a Fluidized-bed Crystallizer," *Kagaku Kogaku Ronbunshu*, **9**, 214-216 (1983a)
- Toyokura, K., T. Ueno, M. Uchiyama and M. Kawai; "Effect of Seed Crystal Size on Secondary Nucleation Rate of K-alum in Agitated Fluidized Bed Crystallizer," *Kagaku Kogaku Ronbunshu*, **9**, 569-571 (1983b)
- Toyokura, K., S. Yoshida, T. Mano and M. Uchiyama; "Growth of Barium Hydroxide Octahydrate Crystal," *Ind. Crystallization* '84, 285-288, ed. by S. J. Jancic and E. J. de Jong, Elsevier Science Pub., The Netherlands (1984)
- Toyokura, K., S. Takeuchi and H. Sakai; "Effect of Suspended Crystals on Effective Secondary Nucleation in Supersaturated Solution," *Proc. of World Cong. III, of Chem. Eng. II*, 1020 (1986)
- Toyokura, K., O. Morooka and T. Ueno; "Growth of Calcium Sulfate Dihydrate Needle Crystals," *Kagaku Kogaku Ronbunshu*, **13**, 216-222 (1987a)
- Toyokura, K. and E. Sakai; "Design Chart and Industrial Application," *Seminar on Ind. Crystallization in Japan*, **87**, by Czech. Academy of Sci. (1987b)
- Toyokura, K. and K. Ohki; "Size Distribution of Needle Crystals of Urea Obtained From CMSMPR Crystallizer," *Kagaku Kogaku Ronbunshu*, **15**, 817-823 (1989)
- Toyokura, K., S. Akaishi and K. Sase; "Growth and Breakage of Needle Calcium Sulfate Dihydrate Crystals," *Gypsum & Lime*, **226**, 127-134 (1990a)
- Toyokura, K.; "Fundamental Series of Food Engineering, Bunri to Seisei," edited by Yano, T. and Toei, R., Pub. Kohrin, Vol.8, 221-282 (1990b)
- Yokota, M. and K. Toyokura; "Generation Rate of Fines Crystals in Supersaturated Solution of DL-SCMC with NaCl and Adhering Rate of Fine Crystals to Seed Crystals," *Kagaku Kogaku Ronbunshu*, **18**, 832-839 (1992)
- Yokota, M. and K. Toyokura; "On the Generation Kinetics of D- and L-form Fine Crystals During Preferential Crystallization of s-carboxymethyl-L-cysteine," *Kagaku Kogaku Ronbunshu*, **19**, 1081-1088 (1993a)
- Yokota, M. and K. Toyokura; "Crystal Growth Rate of L-SCMC in Aqueous Supersaturated Solution of L-SCMC with fines," *The Third Korea-Japan Symp. on Sep. Tech.*, 731-734 (1993b)